Precise study of the first deflecting magnet of "Rhodotron" (TT200) using transfer matrices and ANSYS11

Farshid Tabbakh[1)]

(Institute of Nuclear Science and Technology, School of Irradiation Application, Atomic Energy Organization of Iran, North Kargar Av., Tehran, Iran)

Abstract The beam trajectory in the first deflecting magnet of "Rhodotron" TT200 has been analyzed precisely by both optical and simulation methods. We found discrepancies between these two methods at the order of (10^{-3}) for the slit distance and deflecting radius and at the order of (10^{-4}) for the magnetic flux density. The main goal of the paper is beam focusing, considering the angular and momentum dispersion of the particles for the magnet designed by ANSYS.

Key words Rhodotron, deflecting magnets, magnetic sector field, ANSYS11

PACS 41.85.Lc, 07.55.Db

1 Introduction

"Rhodotron"[1, 2] is an electron accelerator with industrial, medical and food irradiation applications. This kind of accelerator has a unique particle trajectory, neither straight like "Linac" nor circular like "Cyclotron". The electrons are accelerated by the electric field produced in a coaxial cavity. After each pass, the electrons are sent back to the cavity to be re-accelerated again by the deflection magnets. The energy of the beam is increased by 1 MeV per each pass. These magnets are not only important for deflecting the beam into the cavity center, but are also important to prevent beam divergence.

In this paper, the first deflecting magnet is studied precisely including its focusing properties and the best geometry of the magnet is also investigated to increase the focusing of the beam. In addition, the simulation results of the beam trajectory by ANSYS11 are included to evaluate the analytical results.

In the next section, considering the fringing field and the effective beam trajectory, the precise values of the deflection radius, magnetic flux density and the real beam trajectory are calculated. In sections 3 and 4 the horizontal focusing of the magnet is studied for the angular and rigidity dispersion respectively including the simulation results.

2 Edge effects (fringing field)

Assuming that the magnetic field lines are in the $-y$ direction, to calculate the magnetic flux density, the bending radius r must be determined considering the fringing field effect. As shown in Fig. 1, considering the effective field trajectory and the outer cavity radius R, the bending radius can be calculated by $r = R\tan 9^\circ/\cos 9^\circ$.

In "Rhodotron" one beam orbit has a length equal to the RF wavelength $\lambda_{\rm RF}$, therefore we have $2R + \frac{1}{4}\lambda_{\rm RF} = \lambda_{\rm RF}$. From Fig. 1 we can find out $R = 1.04$ m and $r = 0.167$ m. Also from Fig. 1, the effective field boundary z^*, and x-displacement of the optical center Δx, can be calculated by the two following expressions[3]:

$$z^* = -z_{\rm b} + \int_{z_{\rm a}}^{z_{\rm b}} \frac{B_y(0,0,z)}{BG}{\rm d}z = -I_1 G/2\,, \qquad (1)$$

$$\Delta x = -\frac{I_2 G^2}{4r\cos^3\varphi}\,, \qquad (2)$$

in which B_y is the magnetic flux density in the y direction as a function of z, B is the effective magnetic

Received 17 December 2008

1) E-mail: ftabbakh2000@yahoo.com

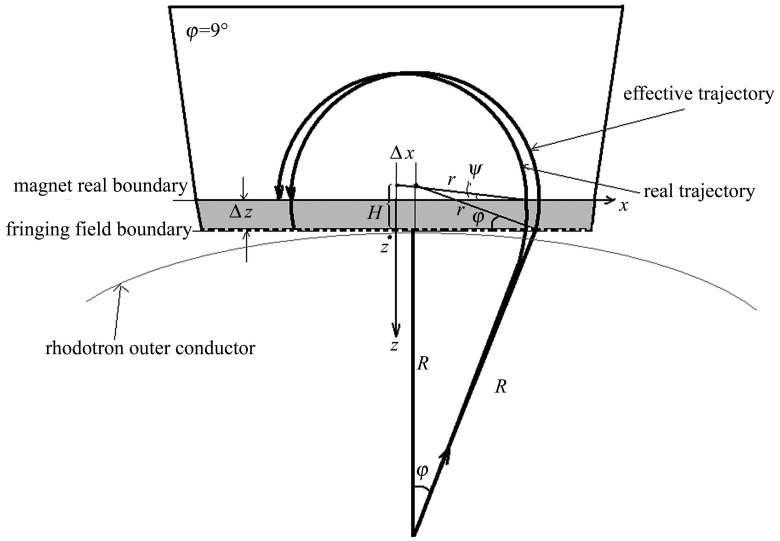

Fig. 1. The real and effective beam trajectories, the displacement of the effective and real optical axis and the beam entering angles.

flux density and $\varphi = 9°$ is the angle between the beam and the vertical direction at the effective field boundary (the incident beam angle at the effective boundary is 81°). The parameters B, z_a and z_b are specified in Fig. 3(b). According to the geometry of the designed magnet, for gap height $G = 5$ cm, the extracted values of I_1 and I_2 are -0.92 and -6.3 respectively, which will give $z^* = 2.3$ cm and $\Delta x = 2.5$ cm[3]. From Fig. 1 the entering angle of the real beam trajectory $\left(\frac{\pi}{2} - \psi\right)$ and the distance between the two slits s are 89° and 33.4 cm respectively. The expected magnetic flux density is calculated by

$$B = \frac{\sqrt{E_k^2 + 2E_k m_0 c^2}}{q_e r c}, \qquad (3)$$

where E_k is the electron kinetic energy, q_e is the electric charge and c is the light velocity. For a reference electron, we have the kinetic energy equal to 1 MeV, $m_0c^2 = 0.511$ MeV, electric charge equal to -1.6×10^{-19} C[4]. Therefore, from Eq. (3) the magnetic flux density will be equal to 0.0284 T.

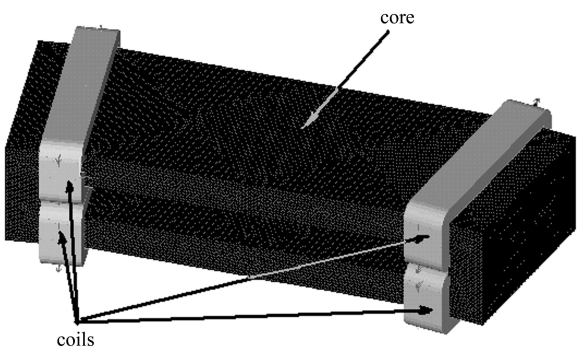

Fig. 2. The core and its 4 related coils of the magnet designed by ANSYS.

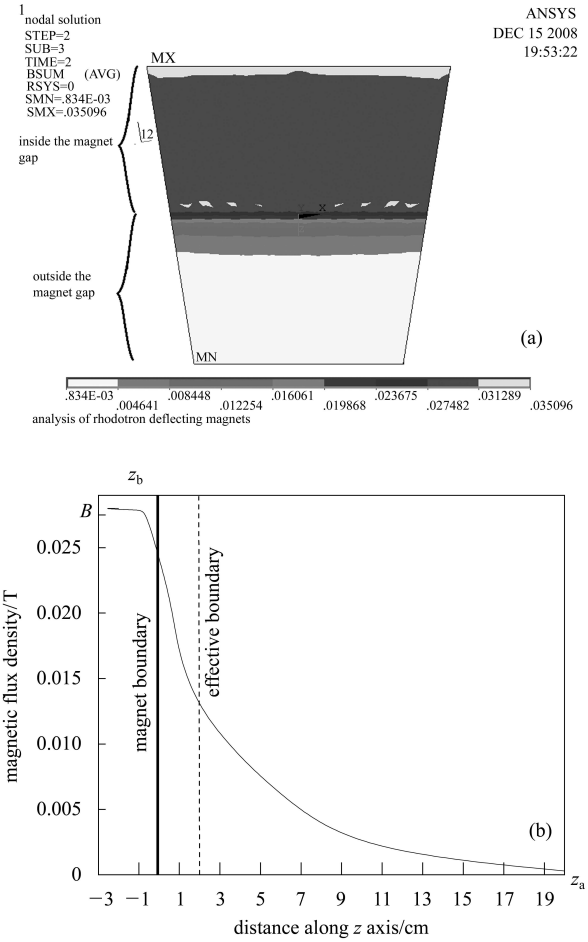

Fig. 3. (a) Distribution of the magnetic flux density inside the gap space obtained from ANSYS simulation according to the designed geometry, (b) distribution of the magnetic flux density along the "z" axis. The magnet boundary is at $z = 0$ and the effective boundary is at $z = 2$.

Applying the 636 Amp turn to the designed coils by ANSYS (Fig. 2) will give us the magnetic flux density $B = 0.0275$ T inside the gap space as presented in Fig. 3(a). After analyzing the 1 MeV electron trajectory, we obtain the parameters $\left(\frac{\pi}{2} - \psi\right)$, r and s as 93.4°, 16.87 cm and 33.7 cm respectively. In addition, Fig. 3(b) shows the simulation results of B as a function of z and then from Eq. (1) we obtain $z^* \approx 2$ cm.

3 Horizontal focusing of the angular dispersion

The different propagating directions of the particles in the beam in a homogeneous magnetic sector field will cause the beam to diverge. To evaluate this divergence, the method discussed in Ref. [3] is used. The transfer matrix and the equations of motion for two particles with incoming deviation angles of α_1 and $\alpha_1' = \alpha_1 + \delta$ from the vertical direction, as shown in Fig. 4, are presented as follows:

$$\begin{pmatrix} D_2 \\ a_2 \end{pmatrix} = \begin{pmatrix} \cos\theta & r\sin\theta \\ -r^{-1}\sin\theta & \cos\theta \end{pmatrix} \begin{pmatrix} D_1 \\ a_1 \end{pmatrix}, \quad (4)$$

$$\begin{aligned} D(\theta) &= D_1\cos\theta + r\delta\sin\theta + \cdots \\ \tan[\alpha_2(\theta)] &= -(D_1/r)\sin\theta + \alpha_1\cos\theta + \cdots \\ \tan[\alpha_2'(\theta)] &= -(D_1/r)\sin\theta + (\alpha_1+\delta)\cos\theta + \cdots \end{aligned}, \quad (5)$$

where θ is the bending angle of the magnetic sector field. Since $\theta = \pi$, the first equation of (5) will be changed to $D_2 = D(\pi) = -D_1$, where D_1 and D_2 are the incoming and outgoing beam diameters.

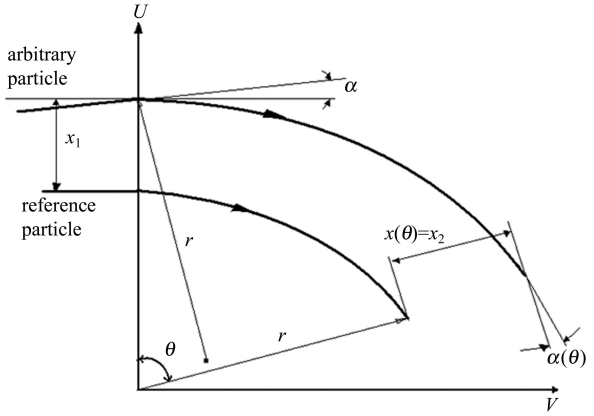

Fig. 4. Two particle trajectories entering a magnetic sector field with bending angle, θ. If α and x_1 are deviation angle and beam diameter at entrance slit, $\alpha(\theta)$ and x_2 are the deviation angle and beam diameter at exit slit.

From the second equation of (5) we have $a_2 = \tan[\alpha'(\pi)] - \tan[\alpha''(\pi)] = -(\alpha_2' - \alpha_2) = -\delta$. This means that the deviation angle will remain intact and in addition it shows that the focusing is just for small deviation angles. As obtained in the previous section, the beam enters the magnet at an angle of $\psi = 1°$ from the vertical direction. The maximum angular dispersion of the beam particles is 0.14°[5]. Therefore, one can conclude that the outgoing beam is focused if the angular dispersion is very small.

The simulation results are presented in Fig. 5. It shows the ratio of D_1/D_2 in terms of the deviation angle ψ. For deviation angles less than 0.2° this ratio is 1.001 and for deviations larger than 0.4°, this ratio will rise.

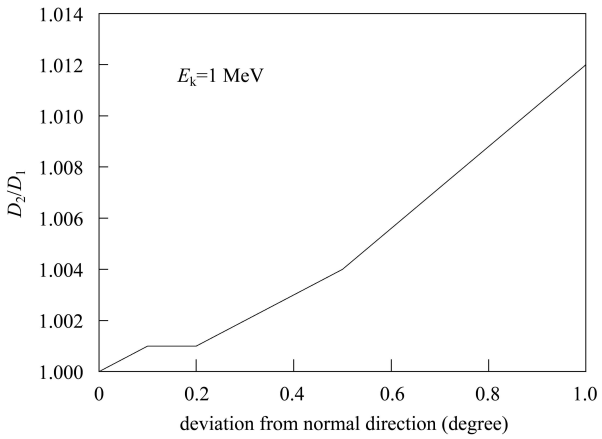

Fig. 5. The ratio of the incoming beam diameter, D_1 and outgoing, D_2 in terms of the deviation angle. This ratio for deviation angles less than 0.2° is almost 1.

4 Horizontal focusing for the momentum dispersion

The transfer matrix for the case of particles with different rigidities (Fig. 6) may be written as follows:

$$\begin{pmatrix} x_2 \\ a_2 \\ \Delta \end{pmatrix} = \begin{pmatrix} \cos\theta & 0 & r(1-\cos\theta) \\ 0 & \cos\theta & 0 \\ 0 & 0 & 1 \end{pmatrix} \begin{pmatrix} x_1 \\ a_1 \\ \Delta \end{pmatrix}, \quad (6)$$

that we have $\Delta = \dfrac{\mathrm{d}r}{r} \neq 0$.

Defining M_x as the lateral magnification and according to the definition of the focusing condition[3] we must have $\Delta r(1-M_x) \leqslant DM_x$ that D is the beam diameter. Substituting x_1 and x_2 with D and DM_x respectively as incoming and outgoing beam diameters in Eq. (6), we will have $-D + 2r\Delta_{\max} = DM_x$. Solving the equation $M^2 + 2M - 1 = 0$ will lead to

$M_x = -2.41$. Finally we can express the focusing condition as a function of the momentum dispersion: $\frac{P_1}{P_0} = 1 + 0.707 \times \frac{D}{r}$. The beam has an "emittance" of 5×10^{-3} cm·rad and therefore the entering beam diameter is about 1.34 cm. Hence, one can expect that for a focused beam, the outgoing beam diameter has to be less than 3.23 cm. The calculations show that for the energy range of 0.98—1.05 MeV (the experimental beam measurements specify some smaller energy range, especially through the first pass[6]) the focusing condition will be satisfied. The magnet focusing power may be written as $-\frac{1}{\Delta_{\max}} = 9.5\times10^{-3}$.

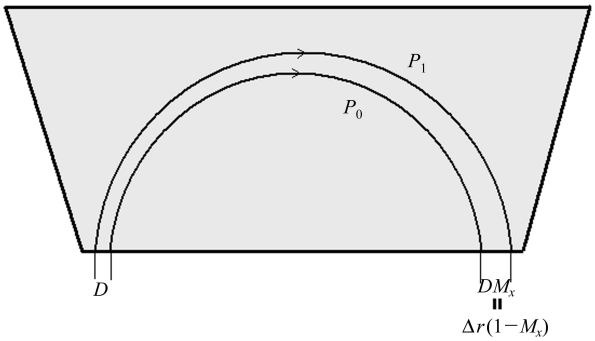

Fig. 6. Two particle trajectories with different momenta, P_0 and P_1. The width of the beam DM_x at the exit slit has to be at least equal to $\Delta r(1-M_x)$.

Figure 7 shows the simulation results of the outgoing beam diameter for particles with an energy range of 0.94—1.05 MeV. Comparing these results with the results obtained from the calculation method, one can see that even for such a wide energy range the focusing conditions are fulfilled.

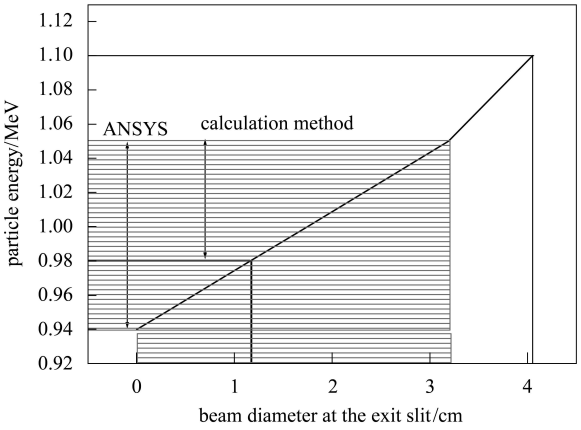

Fig. 7. Beam diameter at the exit slit in terms of the particle energy range.

5 Conclusion

We analyzed the beam convergence in the first deflection magnet of "Rhodotron" TT200 by two methods. The discrepancies between the simulation and the calculation are too small to be considered. For example, the discrepancies for the beam Gyro-radius and the two slits are 0.17 cm and 0.3 cm respectively. According to the experimental measurements of the energy spectra of the beam, the results presented in sections 3 and 4 clarify that the designed magnet satisfactorily focuses the beam during the deflection without any particle loss.

We have to mention that, to increase the beam focusing especially for the magnets of the next passes (because of the wider energy ranges[6]), some modifications can be made to the magnet geometry; this is still under study and will be presented in a future article.

References

1 Pattier J et al. Nucl. Instrum. Methods Phys. Res. B, 1989, **40/41**: 943
2 Umiastovski K et al. Rhodotron: an Accelerator for Industrial Irradiation. Proc. 2nd European Conf. on Accelerator in Applied Res. and Tech. Frankfurt, Germany, 1991
3 Wollnik H. Optics of Charged Particles. Academic Press, Inc., 1987
4 Humphries S Jr. Principles of charged particle accelerator. Department of Electrical and Computer Engineering. Univ. of New Mexico, 1986
5 Gal O, Bassaler J M. Numerical and Experimental Results on the Beam Dynamics in the Rhodotron Accelerator. EPAC, 1992
6 Musavy M, Tabbakh F. E-Beam Spectroscopy of Yazd Electron Accelerator (Rhodotron TT200), RPT-PR-10/77058-RAY/ED-004. Institute of Nuclear Science and Technology, School of Irradiation Application, 2008